Wind Turbine Wakes - Control and Vortex Shedding

by

Davide Medici

March 2004
Technical Reports from
KTH Mechanics
Royal Institute of Technology
S-100 44 Stockholm, Sweden

Akademisk avhandling som med tillstånd av Kungliga Tekniska Högskolan i Stockholm framlägges till offentlig granskning för avläggande av teknologie licentiateexamen torsdagen den 25:e mars 2004 kl 10.30 i seminarierum 40, Teknikringen 8, KTH, Stockholm.

Universitetsservice US AB, Stockholm 2004

D. Medici 2004, **Wind Turbine Wakes - Control and Vortex Shedding**

KTH Mechanics, Royal Institute of Technology
S-100 44 Stockholm, Sweden

Abstract

Wind tunnel studies of the wake behind a model wind turbine have been made in order to get a better understanding of wake development as well as the possibility to predict the power output from downstream turbines working in the wake of an upstream one. Both two-component hot-wire anemometry as well as particle image velocimetry (PIV) have been used to map the flow field. All three velocity components were measured both for the turbine rotor normal to the oncoming flow as well as with the turbine inclined to the free stream direction (the yaw angle was varied from 0 to 30 degrees). The measurements showed, as expected, a wake rotation in the opposite direction to that of the turbine. A yawed turbine is found to clearly deflect the wake flow to the side showing the potential of controlling the wake position by yawing the turbine. The power output of a yawed turbine was found to vary nearly as the square of the cosine of the yaw angle. The possibility to use active wake control by yawing an upstream turbine was evaluated and was shown to have a potential to increase the power output significantly for certain configurations.

An unexpected feature of the flow was that spectra from the time signals showed the appearance of a low frequency fluctuation both in the wake and in the flow outside. This fluctuation was found both with and without free stream turbulence and also with a yawed turbine. The non-dimensional frequency (Strouhal number) was independent of the free-stream velocity and turbulence level but increases with the yaw angle. However the low frequency fluctuations were only observed when the tip speed ratio (or equivalently the drag coefficient) was high. This is in agreement with the idea that the turbine shed structures as a bluff body. It is hypothesized that the observed meandering of wakes in field measurements is due to this shedding.

Descriptors: Wind Energy, Power Optimisation, Active Control, Yaw, Vortex Shedding, Wake Meandering

Preface

The first part of this thesis consists of an introduction to wind energy, its potential and principles, a review of relevant work, a description of the techniques and equipment used in the experiments and a short summary of the results. The second part consists of three research papers which describe the results in detail. The contents of the papers have not been changed as compared to the published versions, except for some typographical errors, but they have been adapted to the present thesis format.

"*Like all other arts, the Science of Deduction and Analysis is one which can only be acquired by long and patient studies, nor is life long enough to allow any mortal to attain the highest possible perfection in it.*"

Holmes, S. (1887) A study in scarlet.

Contents

CHAPTER 1

Introduction

1.1. World energy resources and production

The growing demand of electricity in the world is stressing the traditional sources of energy. For instance, Europe is importing 50% of its energy needs, mainly in form of oil products. An urgent question is how this increased energy demand can be met in an environmentally friendly way. Can wind power provide one answer? The environmental factor is in favour of wind energy because wind is there to use and its use does not produce any green-house emissions.

The principle behind wind energy production is to convert the kinetic energy of the wind into a torque which turns the shaft of an electrical generator. Two limits are obvious: the first is when the turbine is leaving the wind speed unchanged, without extracting any energy. The second is when all the energy of the air that meets the turbine is extracted, however this is not possible since it would mean that the flow has stopped right behind the turbine. The optimal energy production occurs somewhere in between, and it is known as the Betz limit and will be discussed in chapter 2.

The total power in the wind, i.e. the kinetic energy per unit time in the stream tube approaching the wind turbine, is proportional to the cube of the wind speed. This means that the turbine should be elevated as far as possible from the ground, since the velocity in the atmospheric boundary layer decreases towards the ground. The energy extracted is also directly proportional to the diameter of the turbine itself. This factor makes it advantageous to make the turbine as large as possible and has resulted in the development of turbines of increasing size for large scale production.

1.1.1. *The potential of wind energy*

The *rated power* from a turbine (i.e. the maximum obtainable power) is only obtained if the wind speed is higher than a characteristic value, as shown in Fig. 1.1. A typical wind turbine runs below the rated power for approximately 75% of its production time. There is also an upper wind speed above which the turbine is shut down in order to avoid damages to the turbine.

The *installed capacity* of wind energy (for a wind turbine park, country or the world) is the sum of the rated power of all considered turbines. However, the energy produced during a certain time period can only be calculated if also

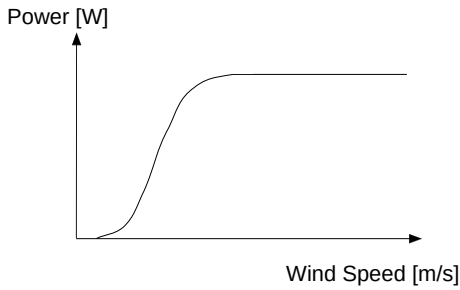

FIGURE 1.1. Power output as function of wind speed for a single wind turbine.

the velocity distribution in time is known for each turbine. Knowing the wind speed distribution, the energy output for a specific turbine can be calculated using a curve similar to Fig. 1.1.

Having the above analysis in mind, in order to understand if wind energy has a potential to develop even further, it is essential to understand the world wind resources. Data have been collected during many years in the 30 OECD (Organisation for Economic Co-operation and Development) countries, which includes Sweden since 1961, and in other areas of the world. The methodology, see for example Grubb & Meyer (1993), is to calculate the available land with an annual average wind speed higher than a chosen threshold value (in the cited case, above 5.1 m/s at a height of 10 m from the ground level). The energy output calculated from the velocity distribution is reduced by 90% when constraints such as high-populated areas, human activities, noise, visual impact, etc. are considered. An estimate of the available wind energy in TWh per year is shown in Fig. 1.3. This estimate refers to what wind turbines were able to produce one decade ago. Today's technology provides higher performances machines. The power of a wind turbine has raised from 0.4 MW at the above cited period to the modern 4 MW machines, manufactured by e.g. Enercon and General Electrics. One example of a modern wind turbine is the Enercon E66 which is shown in Fig. 1.2. It has a rated power of 2 MW and a diameter of 70 m.

Furthermore, no off-shore sites were considered by Grubb & Meyer (1993) whereas, today, great attention is focussed also on this area. For instance, the amount of energy which can be produced by off-shore sites in Europe is estimated in the order of 2000 TWh per year.

1.1.2. *Present world energy use*

When it comes to the statistics of the actual use of energy supplies, there exist small discrepancies between different studies due to differences in the definitions and methods used to evaluate the resources. Here the general definitions

FIGURE 1.2. Enercon E66. Courtesy of Enercon GmbH.

used by the International Energy Agency (IEA, www.iea.org) will be adopted. It states that *renewable energy sources* include hydro, geothermal, solar photovoltaics, solar thermal, tide, wave, ocean, wind, solid biomass, gases from biomass, liquid biofuels, and renewable municipal solid waste. For a more specific definition of each of the above mentioned sources, refer to the report by IEA (2002).

The produced energy in 2001 was $1.2 \cdot 10^5$ TWh[1]. If only electricity production is considered (about 15% of total production), renewables have provided 18% of the world total in 2001.

[1]This value is usually given in toe= tonne of oil equivalent and corresponds to 10038 Mtoe, 1 Mtoe = 11.63 TWh.

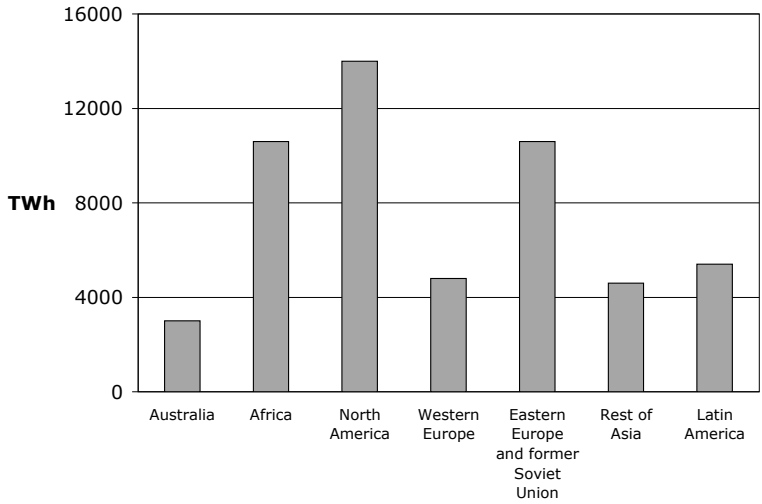

FIGURE 1.3. The world's wind resources, adopted from Grubb & Meyer (1993). The energy available from the wind is 53000 TWh per year.

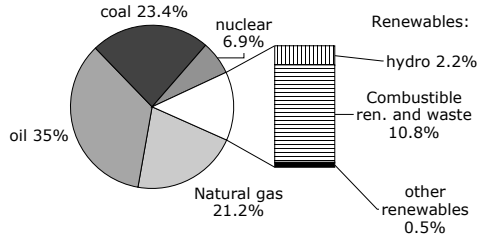

FIGURE 1.4. Fuel shares in world total primary energy supply for 2001 (IEA (2003)).

In the OECD countries, oil provided approximately 41% of the energy supply and renewable sources accounted for 5.7% of the total.[2] The division between the different renewable sources can be seen in Fig. 1.5. Once more, the situation differs for electricity production: renewable sources contributed with 1424 TWh of electricity in 2001, equal to 15% of the production. Wind

[2]The large value of 10.8% in Fig. 1.4 (as regarding the world total) for combustible renewables and waste stem from their heavy use in developing countries.

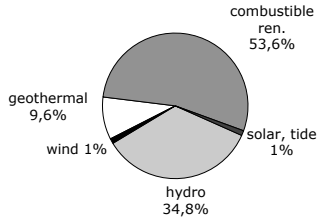

FIGURE 1.5. 2001 products' shares in OECD renewable energy supply, as from IEA (2003).

power contributed with 34 TWh, while hydropower was the main supplier of electricity with 13%. It is therefore clear that only a very small percentage of the wind energy potential is exploited (Fig. 1.3). The updated European situation of installed wind energy can be seen in Table 1.1. Other European countries accounted for 278 MW of installed capacity by June 2003.

Denmark is an interesting example of what can be achieved with wind energy. In Table 1.1, it is noticeable how the installed power capacity in 2003 was relatively small for this country, leader in the world of wind energy. A closer look to the data of Grubb & Meyer (1993) tells us that the theoretical energy production was estimated as 10 TWh. In 2001, Denmark produced

COUNTRY	Installed Jan-Jun 2003 [MW]	Total by June 2003 [MW]
Germany	835	12836
Spain	230	5060
Denmark	36	2916
Netherlands	125	803
Italy	12	800
UK	34	586
Sweden	36	364
Greece	57	354
France	72	220
Austria	80	219
Portugal	21	217
Ireland	0	137
Belgium	12	56
Finland	0	41
Luxembourg	0	16
Total	**1550**	**24626**

TABLE 1.1. European Union Capacity, June 2003. Source: www.ewea.org.

4.3 TWh of electricity by wind power. One may conclude that Denmark is levelling towards its maximum possible installed wind capacity. If so, it would be therefore a "reasonable" estimate to consider the world's energy capability of the order of 20000 TWh, i.e. half of what estimated by Grubb & Meyer (1993).

1.1.3. *Wind turbine parks*

There are several aspects of wind turbines that contribute to the success or are a source of problems for wind energy. One of those is the presence of a power grid able to sustain the loads produced. In order to optimise the resources, wind turbines are often placed in clusters, so called wind farms. The power produced by each wind turbine is usually collected to a common power line and then taken to the local grid. The final power line has to be able to handle the produced power, therefore very remote areas are often not convenient. In Denmark, where the electricity from wind power is approximately 18% of the country's need, the surplus of energy in the electrical grid has been found to be well managed also during very windy days by redirecting the loads on less used sections of the grid. This possibility plays an important role in Europe, since all grids are interconnected and the electricity can be easily directed somewhere else if not used where produced.

The transport of the wind turbine parts during the assembling process or in case of failure of a component should be as effective (and thereby inexpensive) as possible. Nowadays more and more wind farms are built off-shore. The distance from the coast is limited by the length of the power connection, the depth of the sea (typically a maximum of 30 m is chosen) and the accesibility of the site for maintenance operations. Off-shore, problems arise with the presence of less friendly conditions like waves, salt, ice and other seasonal weather conditions. On the other hand, the atmospheric boundary layer is more suitable for use at sea: lower turbulence, i.e. lower loads on the structures, and higher velocity at the same height compared with the boundary layer over the land. These factors entail the possibility for larger turbine diameters and lower towers than for wind turbines on-shore. The public perception is also more friendly since the turbines are further away.

Setting up a wind farm encounters many problems, only partially technical. Some of the logistic difficulties have been mentioned above. An estimate of the cost for installing an on-shore wind turbine is 900 EUR/kW rated power. Differences between on-shore and off-shore are evident in the division of the costs: on-shore 70% is accounted for the turbine itself, while off-shore the proportions are changed with a more costly foundation and an higher total cost, although these values strongly depend on the site. Thanks to the continuous progresses in wind power technology, e.g. the improvement in the design and the increase in size, the cost of the electricity in the last years has quickly fallen, as can be seen in Fig. 1.6. A projection for the short term is also included.

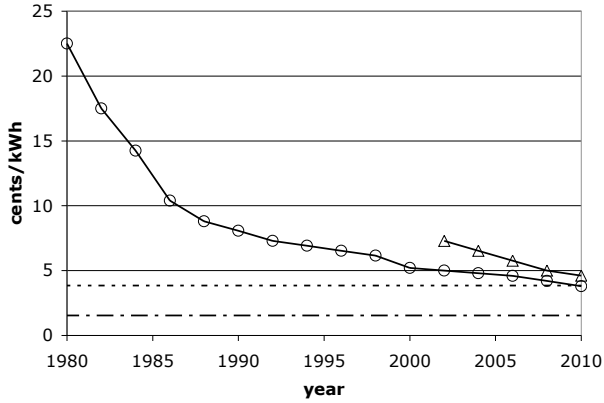

FIGURE 1.6. Production cost per kWh for the largest wind turbines on the market at a given time, from Jones (2003). ◯: on-shore installation, △: off-shore installation. The minimum and maximum market prices are indicatively represented with dashed lines.

1.2. Future development

In the previous sections the potential for wind power has been discussed: the resources are substantial and the technology is allowing their use in competition with other sources of energy. The political determination is crucial for the future. Several organisations are now regrouping in Europe under the *European Renewable Energy Council*. As a part of it, the European Wind Energy Agency not only monitors the development of wind energy, but sets targets for future developments. The predicted goals have always been exceeded by the achievements, as can be seen in Table 1.2.

In year 2000 wind energy contributed in Europe with 0.9% of the electricity production; now the target is to increase the production up to 12.9% by 2020, which will mean 444 TWh in that year (Table 1.2). To achieve this, two future scenarios have been proposed (Zervos (2003)). In the first the annual installation of wind power is assumed as increasing with a steady trend, although lower than what observed in the last five years. The target is set to 75 GW of installed capacity in Europe by 2010. A second more restrictive scenario assumes instead a decrease in the annual installations (compared to the last two years), and a levelling to 3800 MW per year of installed power. The target is set for this case to 60 GW by 2010. In any case wind energy will play a substantial role in the electric energy supply chain.

1.3. Objectives of the thesis

Wind turbines in a park are often placed in parallel lines, with the distance between the lines of the order of 5 to 9 diameters. The orientation is best

year	predicted [GW]	achieved [GW]
1991	4 in 2000	12.8
	100 in 2030	
1997	8 in 2000	12.8
	40 in 2010	
	100 in 2020	
2000	60 in 2010	
	incl. 5 offshore	
	150 in 2020	
	incl. 50 offshore	
2003	**75 in 2010**	
	incl. 10 offshore	
	180 in 2020	
	incl. 70 offshore	

TABLE 1.2. Wind energy capacity in Europe, EWEA targets. Zervos (2003).

when, for the prevailing wind direction, the interaction between the wake from an upstream wind turbine and a downstream one is minimised. The reason is not only that the power extracted is reduced by the velocity defect in the wake, but also the fatigue loads on the structures can become much higher. One objective of the thesis is to give a better understanding of the physical behaviour of turbine wakes by studying the wake behind rotating model turbines in a wind tunnel.

Another objective is to study the possibility of using the already existing yaw control on turbines in order to deflect the wake away from the downstream turbine. With this, loads on the shadowed turbine can be decreased and power production may be improved. The aim is to understand to what extent the side force created by the yawed turbine effects the wake and how the structure of the 3-dimensional wake is changed. An interesting observation is that the the turbine model sheds large scale structures in a similar way as a solid disc. These structures are assumed to be responsible for the meandering of the wake, which has been observed for example in field measurements in the Alsvik wind farm, on the island of Gotland. This kind of motion can be very important in wind parks, where interactions between several wakes can take place.

CHAPTER 2

Wind turbines: principles and design

2.1. Background

When the air flows around a streamlined body such as a wing profile, the pressure field is modified and therefore a force is generated. The component perpendicular to the flow direction is called *lift*, the component parallel to the inflow is the *drag*. The angle of attack between the blades and the direction of the relative wind is not only the result of the wind direction since the blade itself is moving. What happens can be clearly seen in Fig. 2.1 on one of the wind turbine models used for the experiments. The azimuthal velocity must be added to the wind speed, from left.

Some confusion as regarding the drag can arise. The force which is acting on the entire wind turbine in the same direction of the wind, is called drag as well. The application point of this force is the centre of the rotor, if the turbine is aligned with the uniform flow and the tower is neglected. Since the wind turbine studies are traditionally connected with the propeller area, this force is sometimes also called thrust.

For good performance of a wing, the separation of flow on the blade should be avoided. This is the reason why wind turbines have twisted blades: the

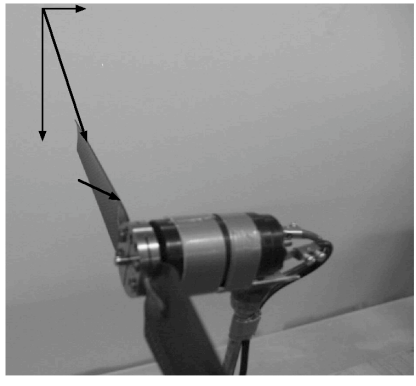

FIGURE 2.1. The angle between the plane of the rotor and the local wind direction is decreasing as moving towards the tip. The stall starts from the root.

angle of attack is optimised from tip to root, for the most frequent operational condition, by making the blade to turn out of the plane of rotation when moving towards the root. However the so-called *stall control*, one of the main aerodynamic controls on wind turbines, makes the stall to occur gradually from the root as the wind speed increases. The reason is to avoid high loads and also high power production which can cause problems to the electrical components of the wind turbine . This is a passive type of control, since the angle of attack on the blades increases with increasing wind speed.

A second important aerodynamic control present on wind turbines is the *yaw control*. It will be shown how the power is proportional to the cube of the wind speed normal to the rotor plane. To maximize the power output the wind turbine is turned towards the wind by means of electrical motors, which move the entire nacelle (i.e. the top part of the wind turbine including the shaft, the gearbox if present, the generator and the other systems) around the tower. Both the yaw control and the twist of the blades were well known in the past, when windmills produced not electrical but only mechanical energy. One example is the Morgan Lewis windmill, Barbados (Fig. 2.2) for which the pole connected to the backside of the "nacelle" was used to turn the blades towards the wind. The system required 10 men to be activated.

The third mostly used control is the *pitch control*. In this active control, the entire blade is turned, to optimise the angle of attack with respect to the wind. If the power output from the generator becomes too high, the system decreases the angle of attack of the blades, in order to obtain less power. This mechanism is the opposite of the *active stall control*, where the blades are instead turned out of the wind to increase the stall, thereby "wasting" the excess energy in the wind.

All the wind turbines have a cut-in wind speed, after which the wind generated torque is greater than the friction in the system and the rotor starts to rotate and produce electricity (see Fig. 1.1). The cut-off speed is instead the higher limit for the working conditions, above which the loads produced are considered dangerous for the machine. The range of velocities is typically somewhere between 3 m/s and 30 m/s, but depends on the type of wind turbine considered. When the conditions exceed the highest velocity limit, the turbine is stopped first by means of aerodynamic controls, e.g. pitching the blade and causing an extended stall, and then the brakes act on the shaft. Tip ailerons are also used in some models as aerodynamic breaks, or the entire tip itself is tilted.

Most wind turbines run at constant rotational speed, giving a constant frequency of the current produced. Small fluctuations in the frequency are allowed and adjusted with an electronic converter. The reason is that the turbines are connected to an electrical grid with a specific frequency of the current (50 Hz in Europe), which has to be matched by the production plant.

FIGURE 2.2. Morgan Lewis windmill, Barbados. The blades move a mechanism used to smash sugar canes. Built in 1727, it shows some technical solutions (yaw control and twisted blades) applied in order to improve its performance.

2.2. Theoretical estimate of power production

It is possible from so called actuator disc theory to establish an upper limit on the power production for a turbine. This is called the Betz limit and it is based on the mass and momentum conservation over a control volume which includes the turbine. Usually this is done by considering a stream tube as shown in Fig. 2.3, where the velocity is assumed to be uniform at each cross section of the tube. In a first approximation the wind turbine can be considered acting like a disc, the *actuator disc*, which has an infinite number of blades creating the needed pressure drop. The velocity along a streamline decreases when approaching the disc and therefore the atmospheric pressure p_∞ raises to the value p^+, according to Bernoulli to balance the velocity decrease. After the discontinuity surface of the actuator disc over which the pressure decreases, the pressure again increases from a lower value p^- to the initial, undisturbed value p_∞. The difference between p^+ and p^- gives the force acting on the disc.

The inflow and outflow boundaries are taken at such a distance that the pressure has recovered to the undisturbed atmospheric pressure (p_∞). The

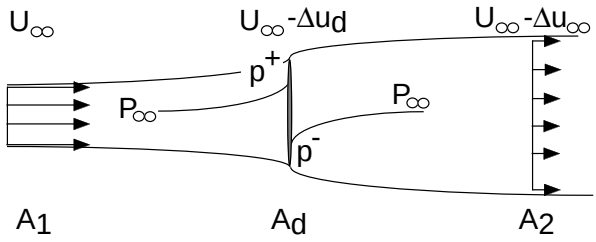

FIGURE 2.3. The wind speed is changed from upstream to downstream due to the presence of the actuator disc, which is represented in the middle of the graph.

power output of the turbine can be obtained in two different ways, either as the change of kinetic energy per unit time between the inflow and outflow boundaries, or as the force (pressure difference across the turbine times its area) times the velocity at the disc.

However, in the literature it is common that the momentum balance is taken over a stream tube of the form seen in Fig. 2.3, which in principle is not possible, since also the varying pressure (which is not equal to p_∞) on the mantle area of the stream tube has to be taken into account. It is possible to overcome this problem by considering a much larger stream tube which includes the one passing over the turbine. If the radius of that stream tube is large enough the pressure disturbance on the mantle surface will decay with the distance (r) from the turbine as r^{-2} and there will be no overall contribution from the pressure forces on the momentum balance. This means that the contribution of the pressure forces on the mantle surface in Fig. 2.3 actually equals $p_\infty \cdot (A_2 - A_1)$, cancelling exactly the pressure force due to the increase in the area at the downstream end of the stream tube.

In order to establish the Betz limit it is necessary to state the equations of conservation of mass and momentum. The mass flow ($\dot{m}$) which runs through the stream tube enclosing the turbine disc can be written

$$\dot{m} = \rho A_1 U_\infty = \rho A_2 U_2 = \rho A_d U_d \tag{2.1}$$

where A_1 and A_2 are the upstream and downstream areas of the stream tube and A_d is the actuator disc area. Using momentum conservation, the drag D on the turbine can, with the arguments used above, be written as

$$D = \dot{m} U_\infty - \dot{m} U_2 = \rho A_1 U_\infty^2 - \rho A_2 U_2^2 \tag{2.2}$$

By using Bernoulli's equation both upstream and downstream the turbine it is possible to obtain an expression for the pressure difference $p^+ - p^-$ across the turbine such that

$$p^+ - p^- = \frac{1}{2}\rho(U_\infty^2 - U_2^2) \tag{2.3}$$

and the drag on the turbine hence becomes

$$D = \frac{1}{2}\rho A_d(U_\infty^2 - U_2^2) = \rho A_d\left(U_\infty - \frac{\Delta u_\infty}{2}\right)\cdot \Delta u_\infty \tag{2.4}$$

where $U_2 = U_\infty - \Delta u_\infty$, i.e. Δu_∞ is the velocity defect in the wake at the downstream end of the stream tube. Using the same notation, Eq. 2.2 becomes

$$D = \dot{m}\left(U_\infty\right) - \dot{m}\left(U_\infty - \Delta u_\infty\right) = \dot{m}\Delta u_\infty = \rho A_d\left(U_\infty - \Delta u_d\right)\cdot \Delta u_\infty \tag{2.5}$$

where Δu_d is the velocity decrease at the turbine plane. A simple comparison between Eq. 2.4 and Eq. 2.5 gives the result known as Froude's theorem:

$$\Delta u_d = \frac{\Delta u_\infty}{2} \tag{2.6}$$

The total power in the wind, i.e. the kinetic energy passing a control area A per unit time, can be expressed as

$$P_{TOT} = \frac{1}{2}\rho A U_\infty^3 \tag{2.7}$$

The power extracted by the wind turbine on the other hand can be written as

$$P_E = \frac{1}{2}\dot{m}\left(U_\infty^2 - U_2^2\right) = \frac{1}{2}\dot{m}\left[U_\infty^2 - (U_\infty - \Delta u_\infty)^2\right] \tag{2.8}$$

which after some algebra can be rewritten

$$P_E = \rho A_d\left(U_\infty - \Delta u_d\right)^2\cdot 2\Delta u_d \tag{2.9}$$

The maximum power output is found by searching for the maximum in P_E with respect to the velocity defect at the disc Δu_d. From Eq. 2.9 we obtain

$$\frac{\partial P_E}{\partial \Delta u_d} = 0 \rightarrow \left(\Delta u_d\right)_{P_{Emax}} = \frac{U_\infty}{3} \tag{2.10}$$

The maximum power for the actuator disc with no losses, from Eq. 2.9 using Eq. 2.10, can be compared with the energy per time of the wind (Eq. 2.7) in order to obtain the efficiency of a turbine (Betz limit):

$$\frac{P_{Emax}}{P_{TOT}} = \frac{\frac{8}{27}\rho A_d U_\infty^3}{\frac{1}{2}\rho A_d U_\infty^3} = \frac{16}{27} \tag{2.11}$$

The drag and power are often expressed in terms of the non-dimensional drag coefficient C_D and the power coefficient C_P

$$C_D = \frac{D}{\frac{1}{2}\rho A_d U_\infty^2} \tag{2.12}$$

$$C_P = \frac{P}{\frac{1}{2}\rho A_d U_\infty^3} \tag{2.13}$$

In the Betz limit they become $\frac{8}{9}$ and $\frac{16}{27}$, respectively. For a real turbine both C_D and C_P varies with the tip speed ratio (λ), which is the ratio between the tip speed and the free stream velocity. We define it here as

$$\lambda = \frac{\Omega \cdot R}{U_\infty} \tag{2.14}$$

where Ω is the angular velocity of the turbine and R is the turbine radius.

2.3. Design

For modern wind turbines the rotor is often upwind with respect to the tower: loads on the blades created by the passage through the wake of the tower are avoided, as well as noise production. The blades are slightly tilted off the vertical plane, so that on the lower side the distance to the tower is increased to avoid a crash in case a strong wind bends the blades back. Two main concepts are presently on the market: the most common is connecting the shaft with an high speed generator through a gearbox which increases the rotational frequency, as in Fig. 2.4. Without the gearbox the stator is a large multi-layer ring, where the lower rotational frequency of the rotor is balanced by a greater number of poles in the stator. In this way the frequency of the produced current is increased and the machine can be directly connected to the electrical system.

For a given power output, the choice is then between a large, low speed rotor, or a smaller, high speed rotor, although hybrid system have been developed. Ultimately, both have some inconvenience. The weight of the nacelle is of the order of 3-400 tons for the gearless machine, and only about a fifth when the gearbox is present. Also the initial cost is generally in favour of a high speed generator, however the absence of moving parts is a pro-factor for the low speed generator. The gearbox has to stand the torque from the blades and the fluctuations of the wind speed and direction, which may cause it to break.

In the nacelle a small fixed crane can also be placed to considerably speed up the process of changing internal parts of the wind turbine. When it comes to assembling the machine, some interesting solutions can be seen. On-shore the process is usually easier: the machine is put together *in situ* connecting elements of the tower, of the nacelle and of the service parts (shaft, generator, active power controls, etc.). On the ground, in case of a three-bladed turbine, two blades are connected together and then lifted in front of the nacelle. At the end also the third blade is raised and bolted to the shaft.

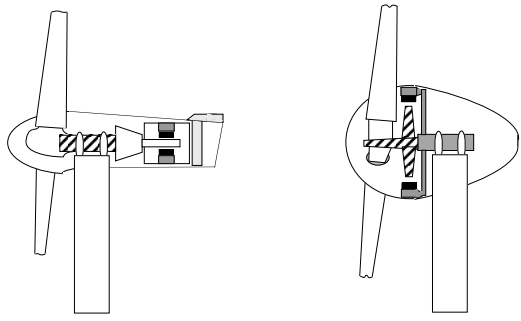

FIGURE 2.4. Figure showing the principles of a turbine with and without gearbox. Left: The gearbox is connecting the shaft, marked with the diagonal lines, and the high speed generator on the right side. At the far right a typical positioning of the cooling system. Right: Gearless machine. From left to right: the blades are connected to the rotor, the magnet (black) and the stator (grey) are visible.

Off-shore the environment is more challenging. First, the basement of the tower must be built. In a second stage, special-purpose ships with a crane are used and equipped with a number of poles which descend on the sea bottom and anchor the ship. On-shore the turbine is put together and then loaded on the ship, for example in only three pieces: the tower, the nacelle with two blades mounted, and a third single blade. The final assembling process of these parts can take place at sea in typical eight hours, if the weather conditions are good enough.

CHAPTER 3

Wind and wakes

In this chapter an introduction to the atmospheric boundary layer and a brief review on wind turbine wakes will be presented.

3.1. Atmospheric boundary layer

A wind farm operates within a region very close to the surface of the earth where the motion of air is strongly affected by a combination of pressure, frictional and Coriolis forces. In this region, called Atmospheric Boundary Layer (ABL), the velocity changes its value from zero at the ground to its full value in the outer part where frictional forces can be considered negligible.

Wind is created by differences in pressure in equal elevation points. These differences are mainly generated by temperature gradients (with associated variations in density) in the atmosphere. Normally neutrally stable boundary layers are considered, for which the influence of the temperature gradients can be neglected while the shear stresses are conditioned by the surface roughness. This assumption can be considered valid for relatively strong winds, which are interesting in the structural design of wind generators. Many reviews on the subject can be found in the literature. See for instance Monin (1970), Tennekes (1972) and Counihan (1975).

Following Monin (1970) it is possible to distinguish different layers within the ABL. The lowest part of the ABL close to the earth surface is called *surface layer*. In this layer the Coriolis forces can be considered negligible. The turbulence can be affected by density stratification which creates buoyancy forces. The effect of the density stratification in ABL decreases when approaching the surface. There is a sublayer, called the *dynamic sublayer*, in which this effect becomes negligible. It is well known that in a turbulent boundary layer on a smooth surface the Reynolds stresses are small compared to the viscous stresses and a viscous sublayer exists. However, land surfaces are always rough enough to force the boundary layer to be highly turbulent down to the surface, and no viscous sublayer can be generated.

Experimental analysis show that the structure of the ABL is very irregular. Such irregularities depend on different factors mainly linked to stratification, non-homogeneity of the temperature field and of course characteristics of the underlying surface. However, measurements show that an equilibrium state can be reached and the flow may become horizontally homogeneous if the wind

blows over an horizontal site of uniform roughness. The thickness can be kept constant due to the horizontal pressure gradient.

In the surface layer the mean velocity profile can be described by the following relation:

$$\frac{U}{U^*} = \frac{1}{\kappa} \ln\left(\frac{z-d}{z_0}\right) \tag{3.1}$$

where U is the mean velocity, U^* is the friction velocity, κ a constant, z the distance from the ground and d a displacement height that for flat surfaces can be set to zero. The term z_0 is a roughness parameter which strongly depends on the terrain considered. Generally very low values of this parameter as well as low turbulence intensities can be found off-shore. Eq. 3.1 is valid approximately till 10-15% of the boundary layer height.

In the upper part of the homogeneous ABL the mean velocity profile can be modelled by the following power law:

$$\frac{U}{U_{ref}} = \left(\frac{z}{z_{ref}}\right)^{\alpha} \tag{3.2}$$

where U_{ref} is the speed at the height z_{ref}, typically 10 m. It can be assumed that this law holds with a constant α up to the top of the boundary layer.

Counihan (1975) collected a large set of data describing the boundary layer parameters in a variety of situations. Turbulence values, power law indices and roughness parameters are listed by type (a city has a much different boundary layer than a rural area) and by site. A wind farm can be influenced by instabilities of the boundary layer, by a nearby forest or by the presence of a hill creating a separation region. The reader can refer to Monin (1970) or more recently to Wizelius (2002) for a more detailed discussion on the subject.

As far as the turbulence characteristics in the boundary layer the scenario is very complicated. In its large-scale limit the atmospheric turbulence approaches two-dimensionality, while its smaller scale forms are inherently three-dimensional. Normally, fluctuations of periods less than about one hour are considered as turbulence. Turbulence profiles are quite variable and depend on the terrain characteristics.

Important quantities in the ABL are the integral scales. They are basically a measure of the average size of the larger turbulent eddies associated with velocity fluctuations. Large eddies result in high correlations at large separations, which thus imply large integral scales. On the average the integral scales decrease with the height from the ground and with the increase of the terrain roughness. Some characteristics of the ABL for different categories of terrain are summarised in Table 3.1.

In wind tunnels there are two methods for the simulation of neutral atmospheric boundary layers. The first involves the use of long and rough surfaces, along which the boundary layer naturally grows. This method gives a good

Category	Type of terrain	z_0 [mm]	α	ABL height [m]
Smooth	ice, snow, sea	5-10	0.12	250
Moderately rough	open grassland	10-100	0.16	300
Rough	forests, suburbs	300-1000	0.28	400
Very rough	city centres	1000-5000	0.4	500

TABLE 3.1. Atmospheric boundary layer data, adopted from Counihan (1975).

representation of the real conditions, but requires very long test sections in order to have reasonable growth. Alternatively, a second method involves the use of artificial devices such as grids which are positioned inside the wind tunnel together with a rough surface accelerating the boundary layer growth (see for instance Talamelli *et al.* (2004)).

3.2. Wind turbine wakes

In this thesis the *wake* is defined as the region behind a wind turbine where the wind velocity has decreased as compared to its value far upstream the turbine. Wakes behind various types of bodies (two-dimensional, axis-symmetric and three-dimensional) have been extensively studied during the history of fluid mechanics. In principle a wake is generated by the loss of momentum due to the force on the fluid by the body (directed in the upstream direction). An equivalent force but with opposite sign is affecting the body itself and this force is usually called the drag force.

The flow characteristics and dimension of a wake depend to a large extent on the geometry of the body. For streamlined bodies the wake is small and of the order of the boundary layer thickness at the aft part of the body, whereas for bluff bodies the size of the wake region may be of the same order as the characteristic cross section dimension of the body. The flow field in the wake is usually highly complex, and depends both on the geometry of the body and the Reynolds number of the flow. For many cases vortical structures are present as a result of instability processes.

However, the wake development can for large downstream distances be described by self-similarity laws, which means that if appropriate variables are chosen, the mean profiles show similarity to each other independent of the downstream position. The self-similarity conditions may, however, depend on the geometry of the body. For instance, it has been shown by Bevilaqua & Lykoudis (1978) that the wake created by two bluff bodies of equal drag but different shapes does not reach the same self-similarity conditions. The reason is that, close to the sphere and the porous disc used in the experiments, different large vortex structures were generated.

As mentioned above instability processes may give rise to vortical structures in the wake. The most well known example is probably the Karman vortex street, which develops behind a circular cylinder if the Reynolds number is above 44. It has also been shown that the shedding frequency can be expressed as a non-dimensional frequency, the so called Strouhal number, which has been found to be constant over large Reynolds number ranges. Also three-dimensional bodies, such as a solid disc, may give rise to vortex shedding. Calvert (1967) showed that circular discs placed normal to the flow gave rise to a specific shedding frequency, however also inclined discs had similar shedding.

A wake behind a wind turbine model is even more complex than that behind a disc or cylinder, since in addition to the already mentioned flow phenomena the turbine sheds strong tip vortices as well as root vortices, giving a periodic upstream boundary condition for the wake. The vortices may also interact and pair with each other further downstream. Since a torque is produced by the turbine, this will also give rise to an overall rotation of the wake.

The wake from a turbine can be divided in two regions: the near wake and the far wake, Alfredsson *et al.* (1980) and Crespo *et al.* (1999). In the former region the wake centreline is constant as moving downstream until the shear layer (i.e. the region of velocity gradient) of the wake has reached the centreline because of turbulent diffusion, typically in 1 to 5 diameters, depending among other things on the ambient turbulence level.

For wind turbine wakes the region behind this initial development is usually called the far wake although self similar profiles are not reached until distances of the order of 30 diameters. As described in Crespo *et al.* (1999), the self-similarity is the basis for the kinetic modelling of wind turbine wakes. The review takes into account both single wake and wind farm modelling. A survey of the methods used to model wind turbine wakes can also be found in Leishman (2002). Experiments are often used to tune the modelling results.

In some cases discs have been used to simulate the wakes of wind turbines in wind tunnels, as e.g. in Sforza *et al.* (1981). The authors claim that matching the tip speed ratio of a wind turbine with a smaller model would change the flow-field characteristics because of the high rotational speed. Therefore these measurements focus on the drag coefficient. The same pressure drop as through a rotor is created by means of porous discs, which also avoid a large separation region. Several drag coefficients have been tested by changing the disc porosity. On the other hand a wind turbine has some characteristics which can be reproduced only by a rotating model, such as the tip vortices, the asymmetric induced velocity field in yawed conditions (e.g. as described in Schepers (1999)) as well as the overall wake rotation.

Experiments on rotating models are usually performed on one turbine or maximum two (Vermeulen (1980), Dahlberg & Medici (2003)) mainly because of the limited space in the wind tunnel. An exception to this is the simulation of a wind farm by Corten *et al.* (2003). They used 24 rotating turbine models, where the power output was measured and optimised

CHAPTER 4

Experimental Methods

4.1. Wind tunnels

4.1.1. *MTL wind tunnel (KTH)*

The Minimum Turbulence Level (MTL) wind tunnel at KTH Mechanics, was used in most of the experiments in this work. The tunnel (Fig. 4.1) is a closed-loop circuit, temperature controlled facility with a velocity speed up to 69 m/s. The test section is 7 m long, 1.2 m wide and 0.8 m high. The roof height of the test section can be adjusted in order to obtain a zero pressure gradient along the test section. The velocity variation achieved along the test section was less than 0.6% of the velocity measured by a Prandtl tube at 8 m/s. The Prandtl tube was placed for these experiments at approximately 1 m from the beginning of the test section, and provided the reference velocity for the calibration of the hot wire, as will be described in more detail later. A slot running along the test section length, in the middle of the roof, allows the access of the arm of the traversing system. With the addition of a wing spanning the full tunnel width, 5 degrees of freedom are possible. Added to the spatial x, y, z (i.e. respectively streamwise, vertical and spanwise) are the rotation around the probe axis and the rotation around the y-axis. A photograph of the test section can be seen in Fig. 4.2.

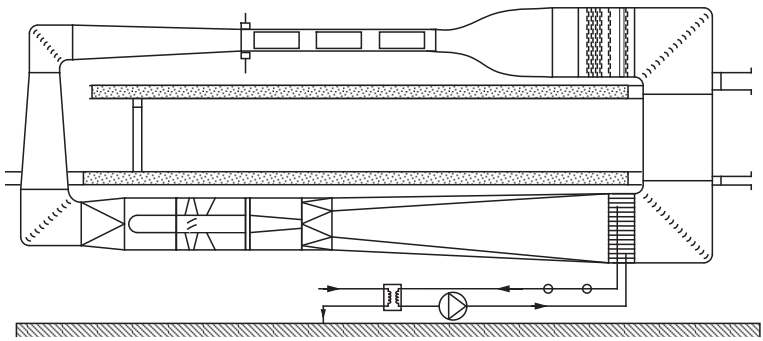

FIGURE 4.1. The MTL wind tunnel layout. The total length is about 25 m and the height is 9 m. The flow is anti-clockwise.

FIGURE 4.2. Test section with traversing system as seen from upstream.

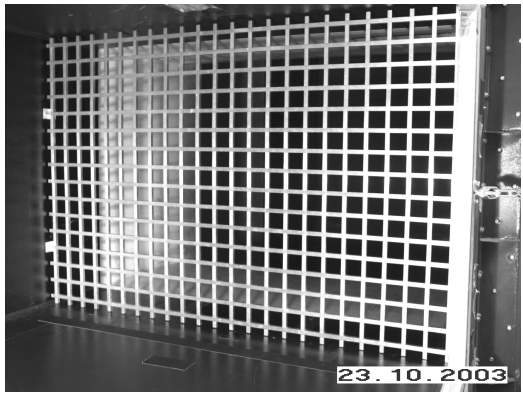

FIGURE 4.3. Turbulence generating grid used in the present experiments.

For some experiments free stream turbulence was generated by the grid shown in Fig. 4.3. The grid was fixed to the tunnel walls 0.2 m after the beginning of the test section, creating a turbulence intensity of approximately 4% of the free-stream velocity at the turbine position. The turbulence intensity for the three velocity components as percentage of the free-stream velocity is plotted in Fig. 4.4 as function of the downstream distance in mm. Without the grid generating the turbulence, the value of the fluctuations in the streamwise direction was less than 0.1% of the velocity measured by the Prandtl tube at 8 m/s.

A heat exchanger gives a very stable temperature control with an accuracy of ± 0.5 degrees by means of water cooling. The temperature is set manually

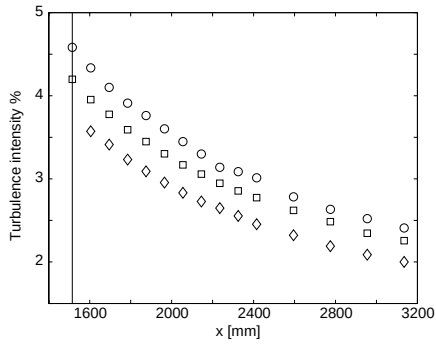

FIGURE 4.4. Turbulence intensity at the test section centre as function of downstream distance for the grid shown in Fig. 4.3. the grid is placed at x=200 mm and the vertical line in the figure represent the position of the turbine. ◯: u_{rms}, ◇: v_{rms}, □: w_{rms}.

at the control panel of the tunnel. Both the tunnel velocity and the traversing system are controlled by Labview programs. Also the data acquisition routines are Labview controlled. For more details about the MTL wind tunnel, the reader is referred to Lindgren (2002).

4.1.2. *LT-5 wind tunnel (FOI)*

The LT5 wind tunnel at FOI were mainly used for the drag interference measurements reported in **paper2**. Figure 4.5 shows the test section, the flow is from right to left. This open-loop wind tunnel has a test section 2.5 m long, with a cross section of 0.9m×0.675m. The velocity range is between 5 m/s and 16 m/s, and the tunnel is run by a centrifugal fan downstream of the test section. At the intake section, a grid helps to reduce the turbulence level. After a short contraction, the test section starts and the turbulence level is approximately 0.3% the free-stream velocity. The wind speed in the centre of the test section is found as the difference between the total pressure in the contraction and the static pressure given by four pressure taps, two upstream and two downstream the model position.

4.2. Measurement techniques

For the wake measurements, two techniques have been used: Particle Image Velocimetry (PIV) and hot-wire anemometry. In the described experiments, PIV gave an overall picture of the flow whereas the mean flow statistics were measured with hot-wire anemometry. Below follows a short description of the present set-ups for these two techniques.

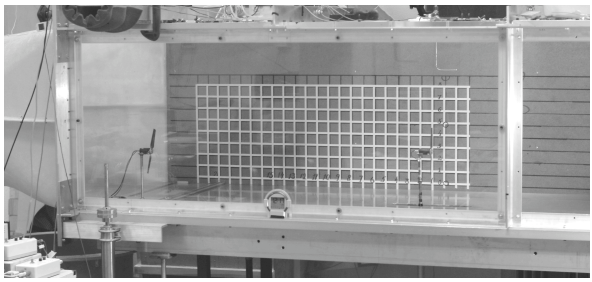

FIGURE 4.5. The test section of the LT5 wind tunnel at FOI.

4.2.1. *Particle Image Velocimetry*

The principle of PIV is simple: the speed of a particle is equal to the distance travelled during a certain time. If particles are added to the flow and they follow the flow, recordings of the particle paths allows us to study the velocity field.

In the present experiments the particle motions are recorded with a CCD camera where a laser sheet perpendicular to the camera lights the flow, i.e. the particles are imaged in one plane. The movements of the particles are registered between two times, t and $t + \Delta t$, where in the present case Δt is typically of the order of 100 μs. In this way the particles are allowed to move somewhere between 0.1 and 1 mm. The post-processing software divides the image in several rectangular regions, the so-called *interrogation areas*. In each of these areas the particle positions between the two recordings are correlated, resulting in the most probable displacement vector (Fig 4.6) during the time Δt.

Some of the factors which have to be set for each type of experiment are the choice of the particles and the time delay between the recordings. The particle size, the concentration in the fluid and body forces on the particles (if in very low speed flows) must also be considered in order for the particles to properly track the flow. In our experiment, propylene glycol oil with an average particle diameter of about 2 μm has been used to seed the flow, together with a 400 mJ Nd:YAG laser as the light source. The time between the two recordings has to be short enough so that only few particles exit the interrogation area. Such a particle has an effect on the signal-to-noise ratio, since its "true" correlated position is not detected. A reliable cross-correlation requires a minimum of 5 particles per interrogation area, and the size of the particles should be at least three pixels on the image in order to pick its correct position. As a rule of thumb the estimated displacement of a particle should not exceed 30% of the side length of the interrogation area. Measuring in regions with large velocity gradients can be a source of problems, since the output vector is an average over the interrogation area (therefore the gradient may be somehow smeared)

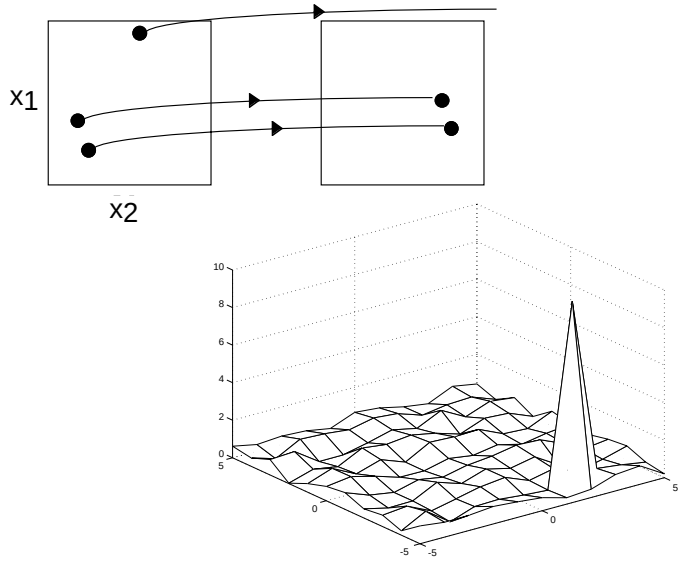

FIGURE 4.6. The correlation principle used in PIV. The sequel of two images from the CCD camera gives the most probable displacement vector in each interrogation area.

and the time chosen for the capturing should be different for different regions of the layer.

The acquisition frequency is mainly imposed by the frequency of the laser. In the experiment here discussed, this value is 14 Hz, which is also the frequency between each pair of images. The CCD camera has 1018×1008 pixels, and was divided in interrogation areas with 64×64 pixels. The side of each interrogation area is 2.7 mm, which is therefore the spatial resolution achieved with the PIV.

4.2.2. *Hot-wire anemometry*

Hot-wire anemometry is a technique where a thin wire (e.g. 5 μm in diameter and 1 mm long) of platinum is heated up to 100-200 degrees above the ambient temperarure. In Constant Temperature Anemometry (CTA) the wire is the fourth arm of a Wheatstone bridge. Depending on the local speed experienced by the wire, its resistance changes, and so does the voltage needed to balance the bridge. The voltage is a function of the velocity value, and the law describing this relation for one-component velocity measurements is known as the *modified King's Law*, see Johansson & Alfredsson (1982):

$$U = k_1(E^2 - E_0^2)^{\frac{1}{n}} + k_2\sqrt{E - E_0} \tag{4.1}$$

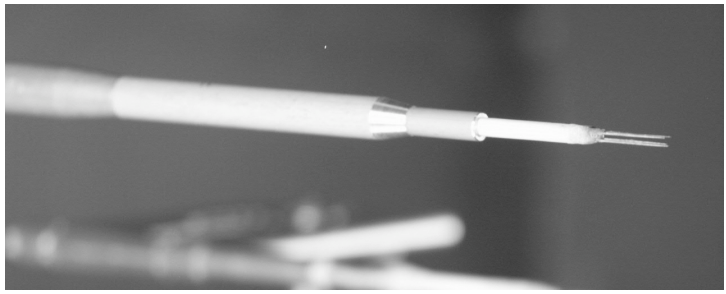

FIGURE 4.7. One of the X-wire used in the experiments. The flow is from right and the measuring volume is a cube with a side length of 1 mm.

where E is the measured voltage, E_0 the voltage at zero velocity, and k_1, k_2, n are the coefficients from the calibration. The wire is soldered to two prongs which are shaped in order to reduce their influence on the flow.

Using two wires placed approximately 45 degrees with respect to the flow direction, the two velocity components can be calculated as combination of the voltages output from the wires. In the calibration, the probe is turned to a known angle (from –40° to +40°) with respect to the free-stream velocity (from 1 m/s to 18 m/s) measured by a Prandtl tube. Two 2-dimensional fifth order polynomials are fitted to the voltages and the coefficients are calculated with the least square method. A typical calibration map is shown in Fig. 4.8.

Calibration points were taken down to a free stream velocity of 1 m/s. If lower velocities need to be measured by the hot-wire, this is not a problem when the modified King's law is used. The polynomials must instead include the velocity range of the measurements. The reason is that the fitting polynomials are not reliable outside the calibration range, since they can diverge to infinity. A solution was found in order to include also the points in the wake, e.g. close to the hub, where the velocity was lower than the allowed minimum of 1 m/s. The voltages from each wire, having in common the same angle with respect to the wind direction, were fitted to the modified King's law. In this way, the voltage values for lower velocities (namely 0.2 m/s and 0.5 m/s) were extrapolated and inserted in the calibration map of the X-wire. Differences were noticeable with the calibration corrected in this way.

4.3. Turbine models

The main advantage of doing simulation of wind turbines in a wind tunnel, as compared to the field measurements, is the controlled flow conditions. On the other hand, the Reynolds number can not be matched: the difference in chord is evident and wind speed must be kept low to avoid too high rotational speed. The latter may be a source of problem, since the centrifugal forces can modify

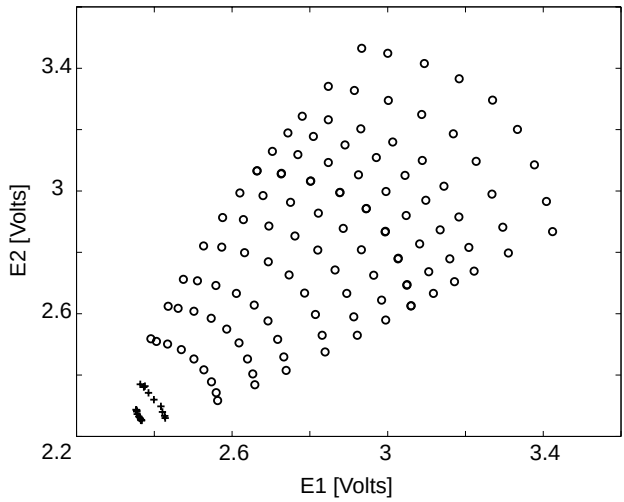

FIGURE 4.8. X-wire calibration map, where the two wires voltages are shown on the abscissa and ordinate, respectively. The circles represent calibration points from 1 m/s to 18 m/s and in 10° intervals with ±40°. The crosses are the values extrapolated using the modified King's law at 0.2 m/s and 0.5 m/s.

the boundary layer on the blades and the development of the wake itself. On the other hand, as mentioned by Vermeer *et al.* (2003), measurements at low Reynolds number are suitable for comparison with numerical models as long as an appropriate wing profile is chosen.

The power output of the turbine can simply be measured from the current and voltage across the generator. However in this case the internal friction as well as losses in the generator are not taken into account. By instead calibrating the generator to obtain the torque from the current its is possible to get the aerodynamic power efficiency.

The drag force measurements were carried out using a strain-gauge balance in the support of the model. When a load is applied, the deformation changes the resistance of the strange gauge. The calibration was made by fixing a known weight acting along the shaft of the generator, where also the rotor acts. The calibration curve can be seen in Fig. 4.9. The weights were measured by a precision balance, with an accuracy of the order of a milligram. The calibration shows a linear relation between the load and the electrical output from the balance.

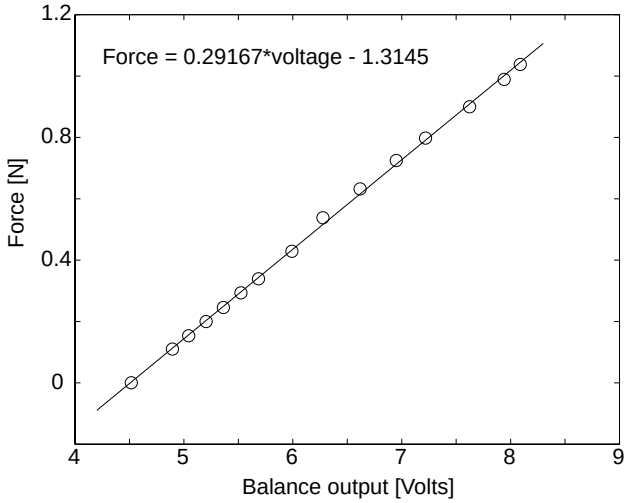

FIGURE 4.9. Drag balance calibration curve with calibration points.

r/R	Chord [mm]	Twist [deg]
0.25	32	15
0.50	35	11
0.75	31	5
1	25	3

TABLE 4.1. Turbine model 1 characteristics.

4.3.1. *Turbine model 1*

The turbine model 1 is used in paper 1. Its diameter is 0.25 m, it has two blades and high solidity (14%). The characteristics of the turbine are shown in Table 4.1.

The nacelle accommodates a generator and the turbine was controlled by a load circuit. This system enabled the change of the rotational frequency keeping the free-stream velocity constant. In this case the power output was calculated as product of the voltage and the current from the generator. The rotational frequency was measured using an optical device fixed under the nacelle, giving an electrical impulse at each blade passage. The turbine was tested at different heights from the floor: 0.248 m, 0.305 m and 0.4 m. No differences were

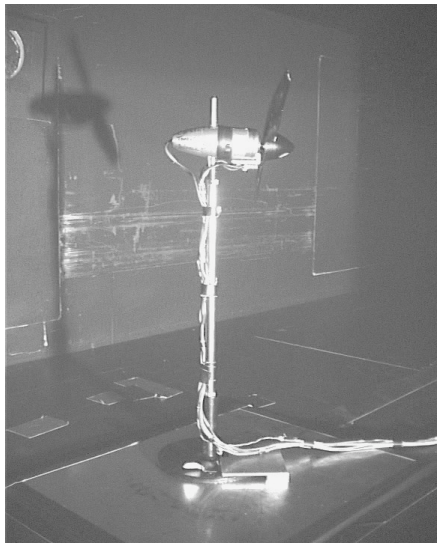

FIGURE 4.10. Turbine Model 1

noticed between these cases, so the chosen height was that with the turbine in the middle of the test section.

The turbine model is shown in Fig. 4.10. When rotating the turbine in yaw, the centre of rotation is directly below the hub of the turbine. The power coefficient for this turbine is shown in Fig. 4.11. The turbine tip speed ratio during the experiments was set such that the turbine operated close to its maximum power coefficient.

When the loading circuit is open, the turbine is free-running: no current flows through the circuit (i.e. no power is produced), and the torque has only to overcome the internal friction of the rotating parts. Therefore the rotational speed is at the maximum value, if the wind speed is kept constant. The open circuit can be achieved by also increasing the variable resistance to a value where the generator is unable to produce a current through the circuit. The opposite situation is when the resistance is zero, or the circuit is short-circuit.

4.3.1.1. *Yaw dependence*

Another characteristic investigated for this wind turbine is the variation of the power with the respect to the flow angle. In Fig. 4.12 the variation both of C_p and the tip speed ratio is shown for turbine model 1. Both the power curve and the tip speed ratio as function of the yaw angle showed a symmetric behaviour after a small offset was applied. The –1.8 degrees offset may be due to an a-symmetry in the turbine behaviour because of the direction of rotation. For this model the variation is nearly proportional to the square of $\cos\gamma$, whereas

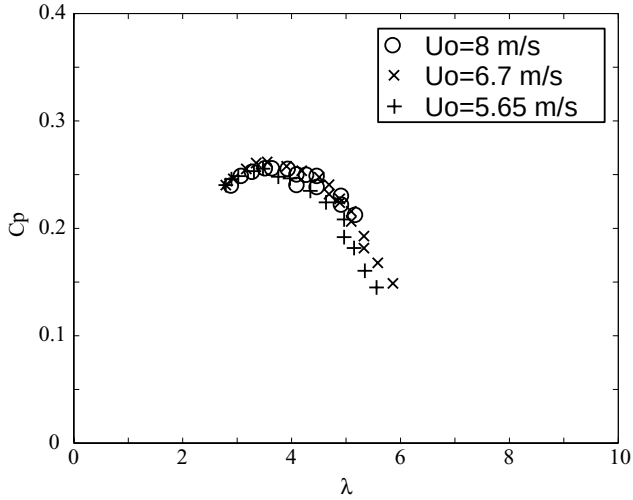

FIGURE 4.11. The power coefficient (C_p) versus tip speed ratio (λ) for three different free stream velocities.

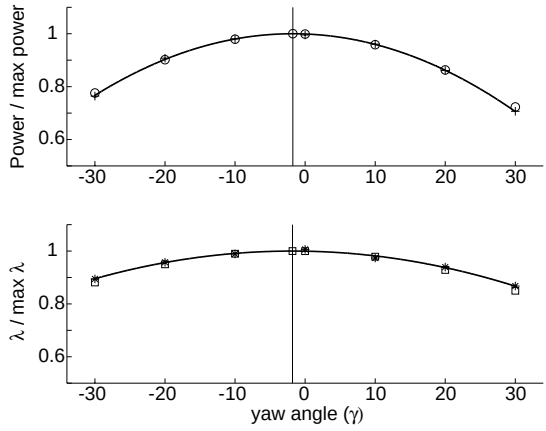

FIGURE 4.12. Power output and tip speed ratio (λ) vs. yaw angle at U_∞=6.3 m/s. The measurement points (+) are normalised with the maximum value obtained from each fitting curve. The squares denotes $\cos\gamma$, the circles denotes $\cos^2\gamma$.

the tip speed ratio varies linearly with $\cos\gamma$ when the loading on the turbine was constant.

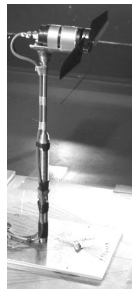

FIGURE 4.13. Turbine model 2.

4.3.2. *Turbine model 2*

A second turbine, built at FOI, was used in other sets of measurements in **paper 2** and **paper 3**. Its diameter is 0.18 m, and as the previous one it is two-bladed. For this turbine the blades are straight (i.e. no twist) and they are built out of four layers of carbon fibres giving a final thickness of 0.5 mm. The profile is based on the Göttingen 417A airfoil, chosen for its good performance at low Reynolds number. The chord at the tip is 16 mm and the maximum chord is 27 mm, at 12% of the radius. The solidity is 13%. The blades are attached by a screw, 3 mm in diameter, to the 23 mm nacelle. These screws allow the setting of the pitch angle of the blades, defined as the line connecting the leading edge to the trailing edge at 85% of the radius. A designated set-up was built at FOI to fix the pitch angle (see Montgomerie & Dahlberg (2003)) and allows an accuracy of ± 0.05 degrees.

The blade pair is connected to a 24V DC motor which works as a generator. In this case the torque was calibrated versus the output voltage and was shown to be a straight line. Hence the aerodynamic power produced by the turbine can be calculated.

The other important characteristic for a wind turbine is the drag[1] coefficient. The results in **paper 2** and **paper 3** show how the drag coefficient first increases with the tip speed ratio and then tends to level out at a value which is of the order of 0.9. During the experiments, the running conditions for the turbine, such as power and drag coefficients, were measured and compared before and after. No change has ever been observed, proving that the model had stable characteristics during the maximum 30 hours measurements period.

[1] As already mentioned the drag of the turbine is sometimes denoted as thrust.

CHAPTER 5

Summary of papers and authors contributions

The thesis is based on the following three papers.

Paper 1
Parkin, P., Holm, R. and Medici, D. "The application of PIV to the wake of a wind turbine in yaw", Proc. 4th International Symposium on Particle Image Velocimetry, Göttingen, 2001.

The experiment was led by PP and RH. The data processing and analysis was done by DM supervised by PP. The paper was written by PP and RH, whereas DM prepared the figures.

Paper 2
Dahlberg, J.–Å. and Medici, D. "Potential Improvement of wind turbine array efficiency by active wake control (AWC)", Proc. European Wind Energy Conference, Madrid, 2003.

The work was equally divided between the authors. The original idea of AWC was by JÅD.

Paper 3
Medici, D. and Alfredsson, P.H. "Measurements on a wind turbine wake: 3D effects and bluff-body vortex shedding".

The measurements were performed by DM, as well as the data analysis. The paper was written together with HAL.

5.1. Summary of papers

In **paper 1** the near wake downstream a rotating wind turbine model is studied using PIV, both with the turbine normal to the free stream direction and under yawed conditions. It is shown that yawing the turbine makes the wake deflect towards the side of the downstream blade, in response to a force perpendicular to the wind direction. The PIV used in the experiment allowed several instant pictures of the flow, and in specific of the tip vortices. The vortices, together with the rotation of the wake, seem to make the difference with the wake from another bluff body, as if the wake can be frozen until these vortices are

particularly strong and easily detectable. The effect of yawing can be seen in the mean velocity values, which are known every few millimetres thanks to the technique used for the measurements. The velocity in a chosen point can even double when the wake moves away.

In **paper 2** various effects on a single turbine under yaw is studied as well as the interaction between two turbines by traversing one turbine in the spanwise direction downstream an undisturbed turbine. In this way a direct measure of the power interference can be obtained, showing itself in terms of "power wakes". The effect of yaw on the power deficit is studied and a model for wind farm is used to predict the effect of active yaw control. It is shown that for a six turbine station an increase in power of about 4% can be achieved.

In **paper 3** the wind turbine wake is studied in more detail using two component hot-wire measurements. It is shown that the wake from a single wind turbine exhibits a large degree of non-symmetry respect to the central axis when yawed. The effect of free stream turbulence is also studied. An unexpected and interesting phenomenon was observed during the measurements, namely a large scale motion of the wake which reflects itself in low frequency variations as detected by the hot wire. The frequency, if expressed as a Strouhal number, is similar to what one would expect for shedding behind a solid disc and it was concluded that the turbine sheds vortices in a similar way as a disc. It was hypothesized that the meandering of the wake observed behind full scale turbines is due to such vortex shedding.

Acknowledgements

I want to thank first my supervisor Prof. Henrik Alfredsson for his guidance and advice which started during my master thesis period at the Lab. Enjoying Science is also experiencing knowledge through someone else (and trying to get as much as possible from it).

Special thanks go to Prof. Alessandro Talamelli for his advise and comments on the thesis.

A very special thanks goes to Jan-Åke Dahlberg. It has been a pleasure to work with a scientist and a friend. I hope to keep the same fun and joy in experiments as you are always able to communicate me. Sven-Erik Thor, Björn Montgomerie and all the FOI wind energy group are also acknowledged for many fruitful discussions and help.

Many special persons in the Lab made my staying here unique: Marcus and Ulf always have the perfect answer (and experimental set-ups) for every question. Dr. Nils Tillmark is acknowledged for his assistance and for his efforts in guiding the Ph-D students crowd toward a well-organised lab. Dr. Fredrik Lundell is the first person I met in Sweden and has been since then a constant reference for advice, friendship and discussions. Dr. Luca Brandt is the second person I met in Sweden and he has been always there for me. Don't ask me who was the third person I met, I can not remember. Many other people need to be mentioned: Jun, Luca F., Jens and everybody in the Lab and at the Department.

Thanks to my brother Dario, to Cesare, Luca S., Guido and to the volleyball team. My life would not be the same without all of you. Someone made a difference: I learned a lot and I will never forget.

Il mio lavoro sarebbe sicuramente diverso senza l'aiuto e l'appoggio che vengono dalla mia famiglia. Posso andare ovunque ma so che un riferimento e' sempre fermo ad aspettarmi. Grazie.

Bibliography

Alfredsson, P. H., Dahlberg, J. Å. & Bark, F. H. 1980 Some properties of the wake behind horizontal axis wind turbines. In *Proc. Third Int. Symp. on Wind Energy Systems*, Copenhagen, BHRA Fluid Engineering, paper J5, pp. 469–484.

Bevilaqua, P. M. & Lykoudis, P. S. 1978 Turbulence memory in self-preserving wakes. *J. Fluid Mech.* **89**, 589–606.

Calvert, J. R. 1967 Experiments on the flow past an inclined disk. *J. Fluid Mech.* **29**, 691–703.

Corten, G. P., Schaak, P. & Eecen, P. 2003 Heat and flux. In *Proc. European Wind Energy Conference and Exhibition*, Madrid, (published on CD).

Counihan, J. 1975 Adiabatic atmospheric boundary layers: a review and analysis of data from the period 1880-1972. *Atmos. Environ.* **9**, 871–905.

Crespo, A., Hernánedez, J. & Frandsen, S. 1999 Survey of modelling methods for wind turbine wakes and wind farms. *Wind Energy* **2**, 1–24.

Dahlberg, J. Å. & Medici, D. 2003 Potential improvement of wind turbine array efficiency by active wake control (AWC). In *Proc. European Wind Energy Conference and Exhibition*, Madrid, (published on CD).

Grubb, M. J. & Meyer, N. I. 1993 *Renewable Energy Sources for fuels and electricity*. Island Press, Washington DC.

IEA 2002 Renewables in global energy supplies, an IEA fact sheet. Technical Report, IEA statistics.

IEA 2003 Renewables information. Technical Report, IEA statistics.

Johansson, A. V. & Alfredsson, P. H. 1982 On the structure of turbulent channel flow. *J. Fluid Mech.* **122**, 295–314.

Jones, D. 2003 Will wind be the energy for tomorrow's generation? In *Proc. European Wind Energy Conference and Exhibition*, Madrid, (published on CD).

Leishman, J. G. 2002 Challenges in modelling the unsteady aerodynamics of wind turbines. *Wind Energy* **5**, 85–132.

Lindgren, B. 2002 Flow facility design and experimental studies of wall-bounded turbulent shear-flows. PhD thesis, TRITA-MEK Tech. Rep. 2002:16, Dept. Mech., KTH, Stockholm, Sweden.

Monin, A. S. 1970 The atmospheric boundary layer. *Annu. Rev. Fluid Mech.* **2**, 225–250.

Montgomerie, B. & Dahlberg, J. Å. 2003 Vortex system studies on small wind turbines. FOI scientific report, ISRN FOI-R–0936–SE.

Schepers, J. G. 1999 An engineering model for yawed conditions, developed on the basis of wind tunnel measurements. AIAA paper 99-0039, 18th ASME Wind Energy Symp., and 37th AIAA, Aerospace Sciences Meeting and Exhibit, Reno, also published in *Collection of Technical papers* (A99-17151 03-44).

Sforza, P. M., Sheerin, P. & Smorto, M. 1981 Three-dimensional wakes of simulated wind turbines. *AIAA J.* **19**, 1101–1107.

Talamelli, A., Riparbelli, L. & Westin, J. 2004 An active grid for the simulation of atmospheric boundary layers in wind tunnel. *Wind and Structures* **7**, in press.

Tennekes, H. 1972 The logarithmic wind profile. *J. Atmos. Sci.* **30**, 234–239.

Vermeer, L. J., Sørensen, J. N. & Crespo, A. 2003 Wind turbine wake aerodynamics. *Prog. Aerospace Sci.* **39**, 467–510.

Vermeulen, P. E. J. 1980 An experimental analysis of wind turbine wakes. In *Proc. Third Int. Symp. on Wind Energy Systems*, Copenhagen, BHRA Fluid Engineering, paper J3, pp.431–450.

Wizelius, T. 2002 *Vindkraft i teori och praktik*. Studentlitteratur.

Zervos, A. 2003 The future of wind energy in Europe. In *Proc. European Wind Energy Conference and Exhibition*, Madrid, (published on CD).